Conference Paper ICPMME 2018

Conference Paper · April 2018

CITATIONS
0

READS
158

5 authors, including:

Bright Kwakye-Awuah
Kwame Nkrumah University Of Science and Technology
30 PUBLICATIONS **273** CITATIONS
SEE PROFILE

Elizabeth Von-Kiti
5 PUBLICATIONS **18** CITATIONS
SEE PROFILE

Isaac Nkrumah
Kwame Nkrumah University Of Science and Technology
20 PUBLICATIONS **111** CITATIONS
SEE PROFILE

Baah Sefa-Ntiri
University of Cape Coast
24 PUBLICATIONS **39** CITATIONS
SEE PROFILE

Synthesis of Zeolites from Bauxite and Kaolin: Effect of Synthesis Parameters on Competing Phases

Bright Kwakye-Awuah, Elizabeth Von-Kiti, Isaac Nkrumah, Baah Sefa-Ntiri, Craig D. Williams

***Abstract*—** Bauxite and kaolin from Ghana Bauxite Company mine site were used to synthesize zeolites. Bauxite served as the alumina source and kaolin the silica source. Synthesis variations include variation of aging time at constant crystallization time and variation of crystallization times at constant aging time. Characterization techniques such as X-ray diffraction (XRD), scanning electron microscopy (SEM), energy dispersive x-ray analysis (EDX) and Fourier transform infrared spectroscopy (FTIR) were employed in the characterization of the raw samples as well as the synthesized samples. The results obtained showed that the transformations that occurred and the phase of the resulting products were coordinated by the aging time, crystallization time, alkaline concentration and Si/Al ratio of the system. Zeolites A, X, Y, analcime, Sodalite and ZK-14 were some of the phases achieved. Zeolite LTA was achieved with short crystallization times of 3, 5, 18 and 24 hours and a maximum aging of 24 hours. Zeolite LSX was synthesized with 24 hr aging followed with 24 hr hydrothermal treatment whilst zeolite Y crystallized after 48 hr of aging and 24 hr crystallization. Prolonged crystallization time produced a mixed phased product. Prolonged aging times on the other hand did not yield any zeolite as the sample was amorphous. Increasing the alkaline content of the reaction mixture above 5M introduced sodalite phase in the final product. The properties of the final products were comparable to zeolites synthesized from pure chemical reagents.

***Keywords*—** bauxite, kaolin, aging, crystallization, zeolites.

I. Introduction

DEVELOPMENT of new materials which are eco-friendly is an aim of present day scientists. With emerging technologies, various materials are being implored to help address important problems existing in all disciplines of science, from the physical end of the spectrum to the biological end i.e. from nanoelectronics to nanomedicine. Zeolites constitute the most important family in microporous family [1]. Traditionally, the term "zeolite" refers to a crystalline aluminosilicate or silica polymorph based on corner sharing TO4 (T = Si and Al) tetrahedral forming a three-dimensional four connected framework with uniformly sized pores of molecular dimensions and are usually considered microporous [1] – [3], [7]. Their porous property has provided it with diverse applications in many different fields. Applications of zeolites include water treatment, ion exchange, detergent production, agriculture, catalysis, construction process, petrochemical cracking and separation of gases and solvents [1], [10], [11]. Other properties such as its uniform pore size or shape, catalytic activity; mobile cation and hydrophobicity or hydrophilicity allows the zeolite to act as multifunctional materials in many industrial applications [5] – [8]. There are naturally occurring zeolites and ones that can be synthesized in the laboratory. However, the synthetic zeolites are preferred to natural zeolite due to the pure crystallinity of its products and also the uniformity of its pore sizes [4]. Alumina and silica are the raw materials used to manufacture zeolite. The potential to supply raw materials for the synthesis of zeolite is unlimited since silica and alumina are among the earths most abundant mineral [5], [14]. In this work zeolite were synthesized from both kaolin and bauxite from Ghana. Procedure for Paper Submission

Development of new materials which are eco-friendly is an aim of present day scientists. With emerging technologies, various materials are being implored to help address important problems existing in all disciplines of science, from the physical end of the spectrum to the biological end i.e. from nanoelectronics to nanomedicine [1]. Zeolites constitute the most important family in microporous family. Traditionally, the term "zeolite" refers to a crystalline aluminosilicate or silica polymorph based on corner sharing TO4 (T = Si and Al) tetrahedral forming a three-dimensional four connected framework with uniformly sized pores of molecular dimensions. Zeolites are usually considered microporous [2], [3], [7]. Their porous property has provided it with diverse applications in many different fields. Applications of zeolites include water treatment, ion exchange, detergent production, agriculture, catalysis, construction process, petrochemical cracking and separation of gases and solvents [8] – [11]. Other properties such as its uniform pore size or shape, catalytic activity; mobile cation and hydrophobicity or hydrophilicity allows the zeolite to act as multifunctional materials in many industrial applications [1], [15]. There are naturally occurring zeolites and ones that can be synthesized in the laboratory. However, the synthetic zeolites are preferred to natural zeolite due to the pure crystallinity of its products and also the uniformity of its pore sizes [15]. In this work bauxite was used as alumina source whilst kaolin was used as silica source in the production of synthetic zeolites zeolite. The potential to supply

B. Kwakye-Awuah is with the Kwame Nkrumah University of Science and Technology, Kumasi, Ghana (corresponding author, phone: 233322060299; e-mail: bkwakye-awuah.cos@knust.edu.gh).

E. Von-Kiti was with the Kwame Nkrumah University of Science and Technology, Kumasi, Ghana (e-mail: vonliz05@yahoo.co.uk).

I. Nkrumah is with the Kwame Nkrumah University of Science and Technology, Kumasi (e-mail: inkrumah.sci@knust.edu.gh).

B. Sefa-Ntiri is with the University of Cape Coast, Ghana (e-mail: bsefa-ntiri@ucc.edu.gh).

C. D. Williams is with the University of Wolverhampton, United Kingdom (e-mail: c.williams@wlv.ac.uk).

raw materials for the synthesis of zeolite is unlimited since silica and alumina are among the earths most abundant mineral [5], [14].

II. Materials and Sample Preparation

Kaolin was sampled from Awaso in the Western Region of Ghana. Sodium hydroxide was purchased from Analar Normapur, UK and distilled water was obtained from KNUST laboratory. Bauxite was sampled from Awaso in the Western Region particularly close to the Ghana Bauxite Company site. The kaolin and bauxite was ground and sieve with 0.75µm under dry conditions.

A. Synthesis of zeolite from kaolin and bauxite

The method used in the synthesis of zeolites from bauxite and kaolin followed our earlier method [15] with slight modifications. 50 g bauxite was digested in 2, 4, 6 and 8 M sodium hydroxide solutions to form sodium aluminate. The process was carried at 130 °C for 5 hours in an electrical oven. The sodium aluminate solution was filtered off the red mud and stored poly propylene containers. A calculated volume of the aluminate solution was added to metakaolin and the mixture was stirred until homogenous slurry was formed. Parameters such as aging time and crystallization temperature were kept constant. However, the crystallization times considered were 5 hours, 18 hours and 24 hours. Variations to the procedure included fusing the metakaolin with NaOH before the addition of sodium aluminate and the addition of extra water. The crystallization times were varied between 5 and 24 hours. No aging was carried out. Crystallization temperature considered was 110 °C for 5 hours. The effect of order of mixing of the reactants on zeolite synthesis was investigated using 24 hours as crystallization time.

In another study the volume and mass of the sodium aluminate and metakaolin were kept same whilst the crystallization times were varied (3, 5, 24 and 96 hours) in the first instance. In subsequent experiments, the Si/Al ratios were varied but crystallization and aging times were kept constant. Finally, the effect of aging (24, 48 and 72 hours) on the phase of zeolite formed was studied at fixed temperature of 100 °C.

B. Characterization of raw materials and zeolite samples

Characterization of the sample became very important to ascertain the composition and the crystal structure of the synthesized zeolite. A PANalytical Empyrean Powder X-ray diffractometer was used to collect data using Bragg-Brentano geometry and a slit configuration of a degree fixed divergence slit of 0.25°. The diffractometer is equipped with a CuKα radiation source (λ=1.5406 Å) and was operated at 40 mA and 40 kV. For phase identification, scans were taken from 2θ = 5 to 80 ° with a step size of 0.013 ° and a scan step time of 8.67 s. Rietveld analysis was then performed using Xpert High Score Plus software.

Using a ZEISS EVO50 scanning electron microscope attached with Energy Dispersive X-ray analyzer (EDX), the morphology of the starting materials and the as-synthesized zeolites were investigated. The SEM was operated on under the following analytical conditions: accelerating voltage EHT = 20.00 kV, Signal A = SE1, WD = 4.0 – 5.5 mm. Bauxite, kaolin and zeolite powder samples were dry sprayed onto aluminium stubs using double-sided adhesive carbon discs. They were then coated with gold to decrease static charging during their observation under SEM conditions. Surface morphology and atomic percentage compositions for the present study were done using EDX. The samples were prepared similarly to SEM for EDX analysis. Instead of aluminium stud, a carbon sample holder was used to avoid errors in the aluminium content and the samples were not coated with gold. A Mattson FTIR spectrometer (Mattson Instruments, UK) equipped with a ZnSe crystal plate attached to the spectrometer with a mercury cadmium telluride A (MCTA) detector and KBr as beam splitter was used to analyze zeolite samples. Measurements were done using 100 scans at 4 cm-1 resolution, units of log (1/R) (absorbance), over the mid-IR region of 1200-400 cm-1. FTIR results were also analyzed using MatLab. Crystallinity of the samples was also deduced from FTIR data. The TG analyses were conducted using a Perkin Elmer thermogravimetric analyzer with an output interface. The raw materials were analyzed by between 25 and 900 °C, using a heating rate of 10 °C min-1. The powdered sample was directly filled into a Pt-Rh crucible for the testing. An amount of between 15-20 mg was used to reduce background noise. Loss in mass and peak temperature were ascertained using TG and TGA curves (derivative TG and second derivative curves).

III. Results and Discussion

Characterization of raw materials

The mineral and chemical compositions of both kaolin and bauxite was analyzed. The chief mineral phase was found to be Gibbsite (99.6 %) and Rutile (0.4 %) in small proportion on performing Rietveld analysis for bauxite. EDX analysis of the kaolin obtained exhibits the presence of Si, Al, Na (Table 1). The percentage of kaolinite mineral was 54.8 % and 45.2 % quartz. The SiO_2 value of 62.64 % was obtained.

Fig. 1 Raw materials (left): bauxite from Awaso bauxite mine, (middle): kaolin from Awaso bauxite mine and (right): kaolin from Anfoega (all in Ghana) used for zeolite synthesis

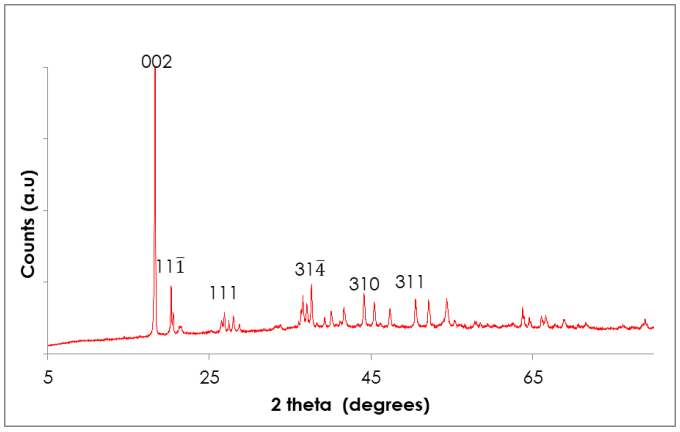

Fig. 2 X-ray diffractograph obtained for bauxite

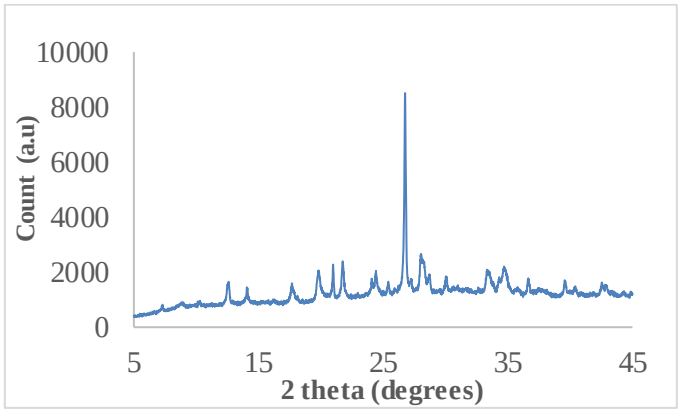

Fig. 3 X-ray diffractograph obtained for Wassa Awaso (blue line) and Anfoega (red line)

Peaks indicating the minerals present in the sample are shown in the XRD patterns (Fig. 2 and Fig. 3). The mineral quartz was significantly present in both samples (according to Rietveld analysis not shown). The percentage of kaolinite mineral was 54.8 % and 45.2 % quartz. An evaluation of the peaks indicate sharp peaks at 2θ = 12.3° and 24.8 °.

TABLE 1
COMPOSITION OF BAUXITE, AND KAOLIN OBTAINED FROM AWASO IN THE WESTERN REGION OF GHANA

Composition	Bauxite	Awaso Kaolin
SiO_2	1.12	56.99
Al_2O_3	88.60	40.97
Fe_2O_3	1.28	-
K_2O	trace	0.54
TiO_2	9.00	
Na_2O	-	1.21
MgO	-	-
Total	100	100

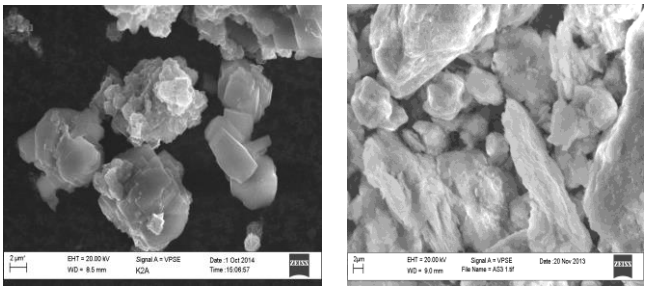

Fig. 4 SEM images for bauxite (left and kaolin samples (middle): Awaso and (right): Anfoega.

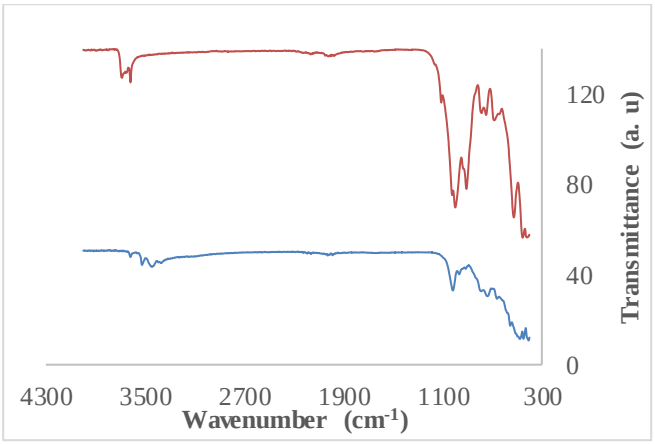

Peak no	1	2	3	4	5	6
Bauxite	473	653	997	3441	3521	3618

Fig. 5 FTIR spectra for bauxite (blue) and kaolin from Awaso (red).

Synthesis of zeolites with varying crystallization time

The XRD patterns of bauxite (Fig. 2) shows the peak positons. The chief mineral phase was found to be Gibbsite (99.6 %) and Rutile (0.4 %) in small proportion on performing Rietveld analysis. The figure shows observable peaks between 2θ = 15° and 55 °. A prominent peak was however observed at 2θ = 18.25 ° with a basal spacing d(002) and a second high intensity peak at 2θ = 20.29 ° and its corresponding basal spacing d(11$\bar{1}$). The EDX pattern showed a high peak for aluminium (Al) whilst the other elements Ti, Fe and K in the compound had relatively low peaks. Silicon (Si) was significantly low as well, as shown in The chemical composition of bauxite presented in Table 1 revealed that Al_2O_3 accounts for 88.6 % wt% of the total bauxite whilst TiO_2, the next highest was 9.0 %, SiO_2 , was 1.28 % and traces of K_2O. A high Al_2O_3/SiO_2 ratio of 79.1 was obtained. Iron impurity was observed to be 1.28 %. No Mg or Fe bearing phase was observed whilst SiO_2 value 62.64 % was obtained from EDX analysis. The SEM of bauxite as depicted in Fig. 4 is somewhat hexagonal but slightly distorted shape. However, the SEM images of kaolin (Fig. 4) show plate-like sheet morphology with a hexagonal outline. The plates are observed to be flaky and loosely packed. Smaller particle sizes are also observed in the image.

The FTIR plot of raw materials (bauxite and kaolin) is presented in Fig. 5. The characterization was carried out between 400 and 4000 cm^{-1}. Similar plots are observed for both kaolins and bauxite. Strong bands at 3618, 3524, 3452 and 3353 cm^{-1} were observed for the bauxite. No prominent peak was observed between 3000 and 1100 cm^{-1}. A number of peaks with variable intensities were observed in the following 1200 – 400 cm^{-1} region. These included 1017, 966, 913, 790, 738, 644, 537 and 529 cm^{-1}. Similar peak positions were noted in the kaolin samples. Peaks at 3664, 3622 and 3613 cm^{-1} were obtained. As with the bauxite, the 1200 - 400 cm^{-1} region had more strong peaks and peak positions were similar to both kaolins. Between 1200 and 900 cm^{-1} region, five bands namely: 1108, 1024, 993, 924 and 904 cm^{-1} band positions were observed. The bands for bauxite compared to kaolin were weaker for this region. In the very low frequency regions, bands were observed around 761, 743, 667, 616, 520 and 448 cm^{-1}.

The SEM images (Fig. 7) show cubic morphology typical of zeolite A crystals. Crystals of zeolite ZK-14 had hexagonal plate-like discs as shown in Fig. 9. Regardless of the mass of bauxite used, similar products were obtained. Zeolite A was the major zeolitic product coexisting with quartz. The quartz peaks were still dominant. Their corresponding zeolite crystallinities were low as peak intensities were not too distinct.

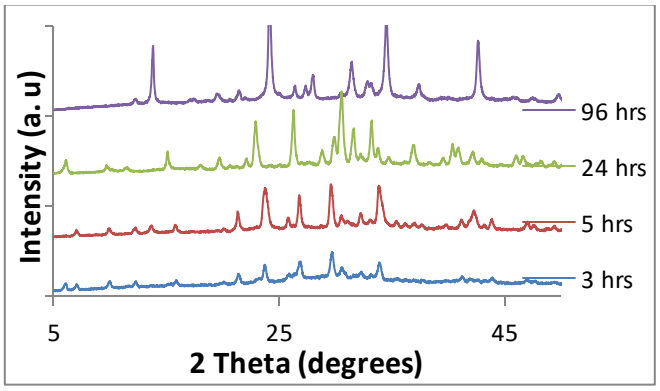

Fig. 6 XRD patterns of zeolites with different crystallization times of 3, 5, 24 and 96 hours.

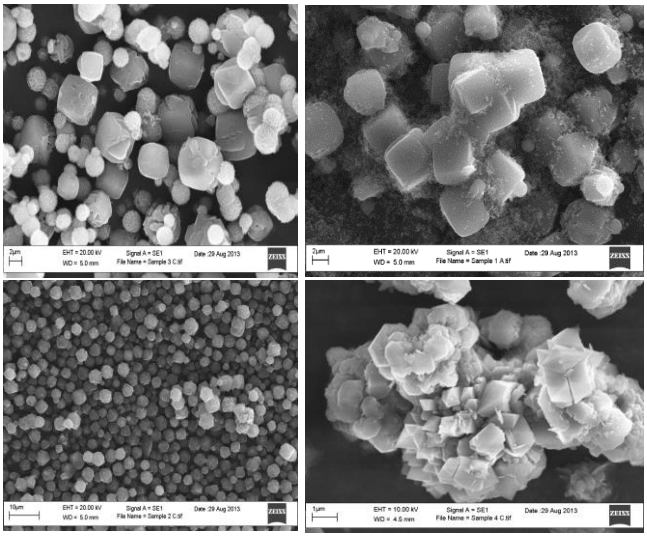

Fig. 7 SEM images of zeolites synthesized at (a) 3 hours (b) 5 hours (c) 24 hours and (d) 96 hours.

The mixed phases observed in the XRD analyses is corroborated by the SEM analyses. The SEM images show mixed species of a cubic formed crystals coexisting with spherical crystals with 3 hours crystallization time. Single cubic crystal cubes are observable in the SEM image after 5 hours. Different particle sizes of zeolite A were however present. Octahedral shaped crystals are portrayed in the image after 24 hours. Wedge shaped crystals were observed after 96 hours of crystallization together with hexagonal disc forming an aggregate.

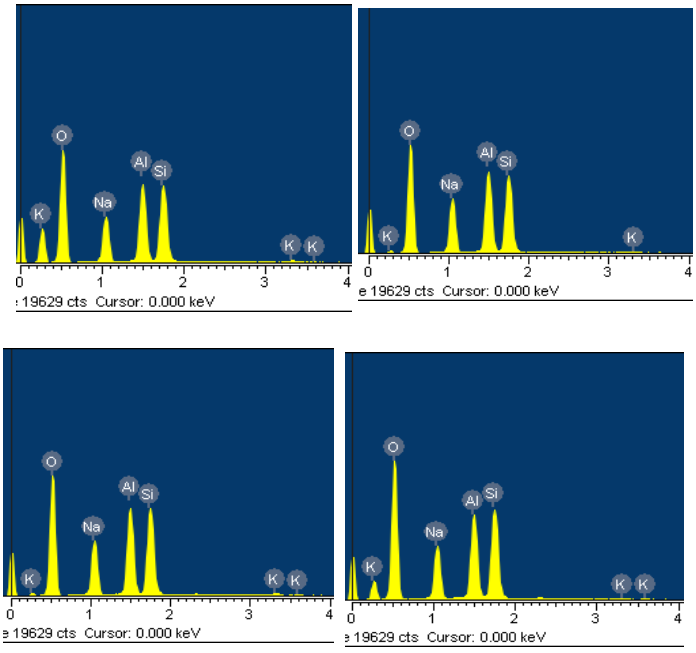

Fig. 8 EDX spectra of synthesized products with crystallization times of (top left) 3 hours (top right) 5 hours (down left) 24hours and (down right) 96 hours.

The EDX analysis of all samples of the synthesized zeolites contained Si, Al, Na and traces of K (Fig. 8). the presence of these ions is an indicator of the recommended ions required in a zeolite structure. The Si/Al ratios in the 3 hours and 5 hours zeolite is ~1 whilst that of the 24 hour zeolite is ~1.3 and ~1.2 for 96 hours.

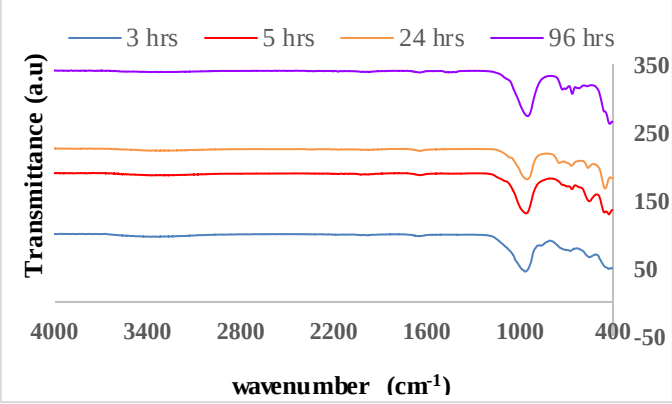

Fig. 9 FTIR spectra of as-synthesized zeolites with different crystallization times.

The results obtained for varying crystallization time is presented in Table 2:

TABLE 2
SUMMARY OF ZEOLITE PRODUCTS PRODUCED FROM VARIATION OF CRYSTALLIZATION TIME

I.D	Aging	Crystal time	Product
1	24	3	Zeolite Na-LTA 62 %, Analcime 27.2 %, Zeolite X 10.9 %
2	24	5	Zeolite LTA 100 %
3	24	24	Zeolite NaK-LSX 93 %, Zeolite Y 7 %
4	24	96	Sodalite 72 %, Zeolite ZK14 16 % Zeolite SAPO 11.7 %

The FTIR spectra in Fig. 9 show similar peak positions for all synthesized zeolites. Highest intensity is observed in the 1200 – 950 cm^{-1} region. Different band positions are observed in the 820 – 750 cm-1 and 650 – 500 cm^{-1} regions. Two broad peaks are noticeable in the 500 – 420 cm^{-1} for the samples synthesized at 24 and 48 hours. The bands assigned to internal vibrations of asymmetric stretching (1250 – 950 cm-1) are found to overlap around 950 cm-1 region. The difference in intensity between the samples (5 hours and 24 hours) in this region can be attributed to the difference in Si/Al ratio. The bands in the 950 – 1250 cm-1 have been studied to be sensitive to Si/Al ratio [19] – [23].

Increasing the crystallization time according to Kovo [10], provides an avenue for the alkalinity content of the system to enhance the solubility of the silicate and aluminate ions resulting in improved poly-condensation reaction between the silicate and aluminate. Generally, the crystallinity and crystal size has been studied to increase with an increase in time. Increasing the temperature of the synthesis mixture has been studied to increase the nucleation rate and the growth rate of the crystal [11], [12]. This implies that higher growth rates results in larger crystals at higher crystallization temperature while lower temperature yields small particle size with a decrease in crystallization rate. Because of the presence of different zeolitic products in the 96 hours sample, a distinct shape could not be identified from the aggregate. However, the Sodalite crystals were quite noticeable (orthorhombic shape). The transformation of zeolite LTA to FAU has been suggested to be due to the basic sodalite cages in both frameworks which form LTA with double 4-rings or FAU with double 6-rings [12], [16].

Synthesis of zeolites with varying aging time

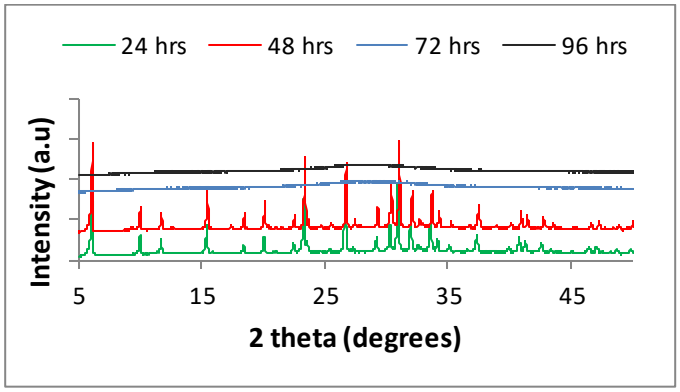

Fig. 10 XRD spectra obtained for different aging times. Aging beyond 48 hours resulted in the loss of crystallinity of the product.

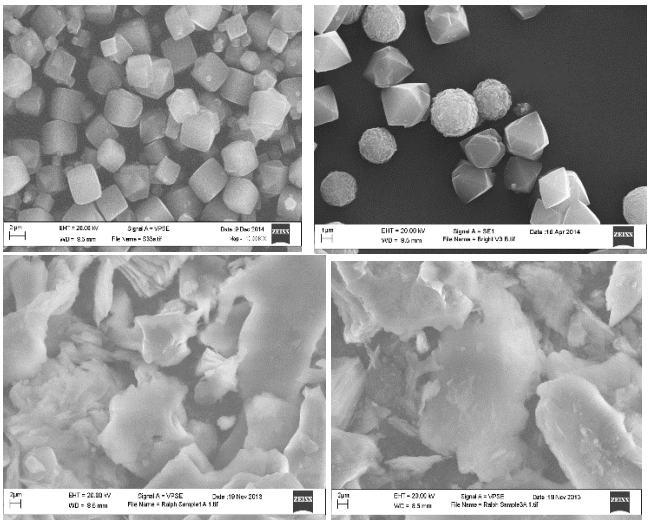

Fig. 11 SEM micrograph for zeolites synthesized with varying aging time.

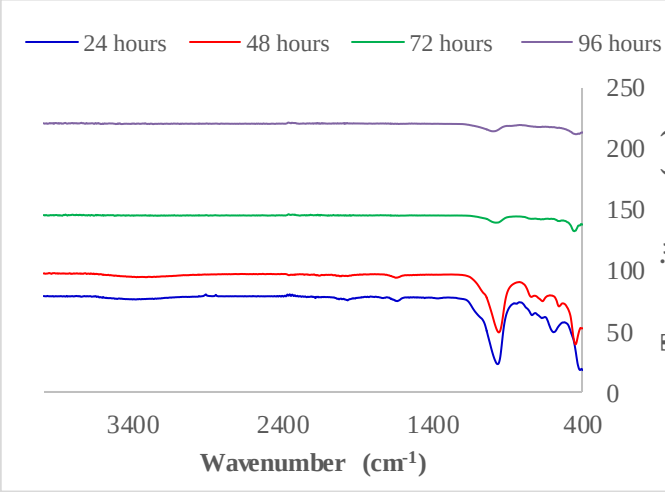

Fig. 12 FTIR spectra obtained for various aging times.

Synthesis of zeolites with varying Si/Al ratio

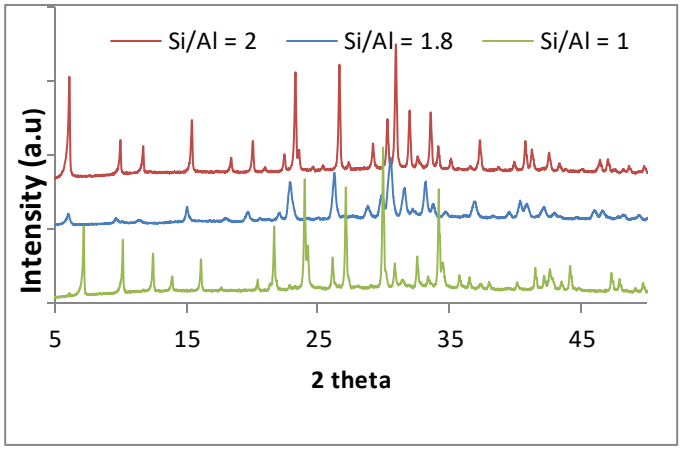

Fig. 13 XRD patterns of the as-synthesized zeolites obtained using varied Si/Al ratios.

Results obtained whilst varying Si/Al ratio with constant and aging times show crystalline products with distinct peaks. First five Peak positions are observed at 2θ = 7.19°, 10.18°, 12.46°, 13.38° and 16.11° for the sample with Si/Al =1 indicating zeolite A (Fig. 13). Similar peak positions are noticed in the samples with Si/Al = 1.8 and 2 but with very high intensity with Si/Al = 2. The first five peak positions are observed at 2θ = 6.12°, 9.98°, 11.7°, 15.4° and 18.37°. These peaks are the characteristic zeolite X peaks. Increasing the Si/Al from 1 to 1.8 produced zeolite X.

Aging of reactants before hydrothermal treatment has been reported to enhance the process by decreasing crystallization time and increasing reaction time. To this effect, aging of reactants for 24, 48, 72 and 96 hours were considered in this study. The solutions were all aged at room temperature. When the aging time was 24 hours, almost pure zeolite LSX was realized and with 48 hours, zeolite Y was achieved.

Nucleation of zeolite crystals is believed to occur during the aging time and remains dormant until an increase in temperature is applied [19] – [20]. Dissolution of silica causing the release of silicate ions is observed with aging of the reaction mixture according Novembre [21], thus increasing the yield and crystallinity of the synthesized product. The formation of FAU is observed with long aging and LTA with short aging [19]. Alkan *et al*. [19] stated that the aging process is necessary for the formation of FAU and also proposed that 6R and double membered rings (D6R) are the precursors of FAU and are formed in the gel phase during the aging process.

Prolonged aging of reaction gels are known to speed up nucleation hence shorter crystallization times will be required for synthesis. Evidence of in different Si/ Al ratio of the crystalline products is depicted by the FTIR with a peak at 967 cm^{-1} for the 24 hour sample and a more intensified peak at 955 cm^{-1} for the 48 hour sample. The crystallinity of the samples is in agreeable with that of the XRD using the intensity of the bands at 554 cm^{-1} and 449 cm^{-1} of the FTIR spectra.

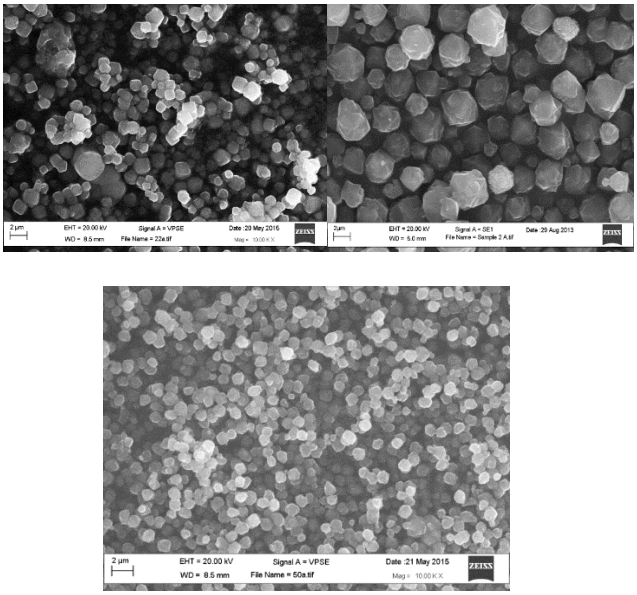

Fig. 14 SEM images obtained for (top left) Si/Al=1, (top right) Si/Al=1.8 and (down) Si/Al= 2.

SEM images (Fig. 14) of the corresponding zeolites confirm the XRD analysis. A cubic outline was seen for the as-synthesized zeolite A. with zeolite X as the product obtained from both Si/Al = 1.8 and 2, a more distinct shape was noted in latter.

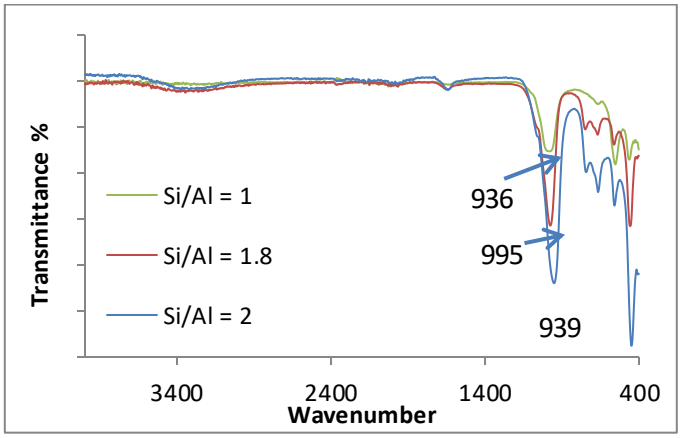

Fig. 15 FTIR spectra of zeolites synthesized with varying Si/Al ratio.

Fig. 15 represent the FTIR spectra of the as-synthesized. An intense band is observed at 936, 995 and 939 cm-1 attributed to as-symmetric stretching of internal vibrations is visible in all three products. The intensity of the bands is however reduced with decreasing Si/Al ratio. A larger number of bands are noticed in the region between 780 and 550 cm-1. These bands are missing in the zeolite A product except for a band at 580 cm-1. Si/Al ratio of approximately 1 produced zeolite LTA. Increasing the Si/Al to 2 under the same conditions, zeolite X was obtained. An increase in Si/Al ratio of the reaction mixture changes the stability of zeolite NaA whilst favouring the formation of zeolite X [22], achieved zeolite X at a higher Si/Al ratio of 2.5 by adding additional sodium silicate solution. The variation in crystallinity of the zeolitic products with respect to aging as depicted by both FTIR and XRD show increased crystallinity with increasing Si/Al ratio. The intensity of the band at 955 cm^{-1} as mentioned previously increases with increasing Si/Al ratio.

Synthesis of zeolites with varying alkali concentration

The molarity of the alkali solution used in obtaining sodium aluminate from bauxite was varied (2, 3, 5, 6 and 8 M). The XRD patterns show crystalline products with distinct peaks (Fig. 16). A similar pattern is observed in the 2 and 3M samples. New peaks appeared with increasing molarity from 3 M to 5 M. The intensity of the peaks also observed to reduce whilst increasing molarity. A similar pattern is noticed in the 5 and 6M samples with similar peak positions. A few peaks were detected in the 8M sample at 2θ = 13.87°, 24.22°, 31.4°, 34.52° and 42.65°. Peak positions of this sample were fairly different from the 2 and 3M however; similar but less prominent peaks were noticeable in the 5 and 6 M products. The SEM images of the as-synthesized zeolitic products using different alkali concentrations. The SEM images were acquired using a working distance (WD) = 2 µm. A cubic crystal morphology is observed in the first two samples (2 and 3 M). The 5, 6 and 8 M SEM images had needle-like crystals coexisting with hexagonal shaped discs. The particle sizes of the crystals appear to reduce with increasing alkali concentration.

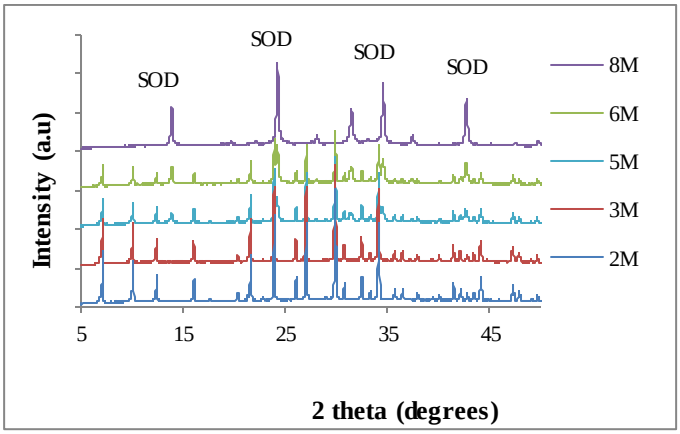

Fig. 16 XRD spectra obtained from variation of alkali concentration.

The ratios of Si/Al of the resultant products are presented in Table 3 below:

TABLE 3
SUMMARY OF ZEOLITE TYPES PRODUCED FROM VARYING SI/AL RATIO

NaOH concentration	Si/Al	Na/Si	Product
2 M	~1	1.1	LTA
3 M	~1	1.21	LTA
5 M	1	1.37	LTA, SOD
6 M	1	1.27	LTA, SOD
8 M	1.06	1.08	SOD

The 2 M, 3 M, 5 M, 6 M and 8 M NaOH concentrations were used to study the effect of increasing alkali concentrations. Upon increasing the alkalinity of solution used during the synthesis of zeolites, a higher yield (mass of final product obtained) was noted to be higher. The final products obtained from reactions are presented in table 5.6

Generally, reaction rate increases with increasing alkaline concentration and a higher yield of the resultant product is usually observed. This is an indication that the dissolution of the solid amorphous phase increases with an increase in the concentration of alkali. Upon further analysis, the best condition for pure zeolite with highest yield was realized at 5M NaOH concentration at 6 hours crystallization time and 100 °C.

Alkan *et al*. [19] synthesized zeolite NaA with kaolin using hydrothermal treatment with 4M NaOH. By increasing NaOH concentrations from 4M to 8M, the ratio of hydrosodalite formation increased in the reaction mixture. With increasing NaOH concentration, Fukui *et al*.[17] observed an increase hydroxysodalite proportion to a decrease in phillipsite mass. Lower mass achieved with lower NaOH can be assigned to

incomplete reaction within the 24 hours crystallization time that was used.

SEM images of the 2M and 3M NaOH concentration samples show well defined cubic crystals confirming pure phased zeolite NaA uniform particle size. Particle size decreased with increasing alkalinity. This can be attributed to

The formation of sodalite at high alkali concentrations from zeolite LTA can also be explained by Ostwald's rule of succession where the first phase to crystallize from a solution will be hydrothermally least stable phase but with time, this phase will transform to a more stable and denser phase [12], [16].

The main band associated with the T-O asymmetric stretching vibrations provide information on the degree of crystallinity of the sample [13].

The intensity of the band was low in the 950 region. This means the crystallinity of this product is low. Band position appearing in slightly higher wavenumbers basically means that the Si/Al ratio of the product is higher.

ACKNOWLEDGMENT

The authors are grateful to Third World Academy of Science (TWAS) for providing a research grant (# 16-471 RG/PHYS/AF/AC_G).

REFERENCES

[1] Breck, B. W. (1974). Zeolite molecular sieves, structure, chemistry and use. New York: John Wiley & Sons.Camblor,

[2] Bhavornthanayod, C., & Rungrojchaipon, P. (2009). Synthesis of Zeolite A Membrane from Rice Husk Ash. Journal of Metals, Materials and Minerals, 19(2), 79–83.

[3] Chandrasekhar, S., & Pramada, P. N. (1999). Investigation on the synthesis of zeolite NaX from Kerala kaolin. Journal of Porous Materials, 6, 283–297.

[4] Coutinho, D., & Balkus, K. (2002). Preparation and characterization of zeolite X membranes via pulsed-laser deposition. Microporous and Mesoporous Materials.

[5] Dodoo-Arhin, D., Konadu, D. S., Annan, E., Buabeng, F. P., & Yaya, A. (2013). Fabrication and Characterisation of Ghanaian Bauxite Red Mud-Clay Composite Bricks for Construction Applications. American Journal of Material Science,

[6] Kloprogge, J. T., Ruan, H. D., & Frost, R. L. (2002). Thermal decomposition of bauxite minerals: Infrared emission spectroscopy of gibbsite, boehmite and diaspore. Journal of Materials Science, 37(6), 1121–1129.

[7] Mozgawa, W., Król, M., Barczyk, K., & Science, M. (2011). FT-IR studies of zeolites from different structural groups. CHEMIK, 65(7), 671–674.

[8] Ruan, H., Frost, R. L., Kloprogge, T., & Duong, L. (2002). Infrared spectroscopy of goethite dehydroxylation . II . Effect of aluminium substitution on the behaviour of hydroxyl units. Spectrochimica Acta Part A, 58, 479–491.

[9] Kovo, A. S., & Holmes, S. M. (2010). Effect of Aging on the Synthesis of Kaolin-Based Zeolite Y from Ahoko Nigeria Using a Novel Metakaolinization Technique. Journal of Dispersion Science and Technology, 31(4), 442–448.

[10] Holmes, S. M., Alomair, A. A., & Kovo, A. S. (2012). The direct synthesis of pure zeolite-A using " virgin " Kaolin. RSC Advances, 44(0), 11491–11494.

[11] Zhu, Y., Chang, Z., Pang, J., & Xiong, C. (2011). Synthesis of Zeolite 4A from Kaolin and Bauxite by Alkaline Fusion at Low Temperature. Materials Science Forum, 685, 298–306.

[12] Criado, M., Palomo, A., & Ferna, A. (2005). Alkali activation of fly ashes. Part 1 : Effect of curing conditions on the carbonation of the reaction products. Fuel, 84, 2048–2054.Chandrasekhar, S., & Pramada, P. N. (1999). Investigation on the synthesis of zeolite NaX from Kerala kaolin. Journal of Porous Materials, 6, 283–297.

[13] Kwakye-Awuah, B., Von-Kiti, E., Nkrumah, I., & Williams, C. (2013). Towards the Zeolitization of Bauxite: Thermal Behaviour of Gibbsite in High-Alumina-Ghanaian Bauxite. International Journal of Engineering Research and Technology, 2(10), 1290–1300.

[14] Kwakye-Awuah, B., Von-Kiti, E., Buamah, R., Nkrumah, I., & C. Williams, C. (2014). Effect of Crystallization Time on the Hydrothermal Synthesis of Zeolites from Kaolin and Bauxite. International Journal of Scientific and Engineering Research, 5(2), 734–741.

[15] Huertas, F. J. (2007). Transformation reactions in phyllosilicates at low temperature: experimental approach. Diagenesis and Low-Temperature Metamorphism. Theory, Methods and Regional Aspects, 65–74.

[16] Alfaro, S., Rodríguez, C., Valenzuela, M. A., & Bosch, P. (2007). Aging time effect on the synthesis of small crystal LTA zeolites in the absence of organic template, 61, 4655–4658.

[17] Fukui, K., Nishimoto, T., Takiguchi, M., & Yoshida, H. (2006). Effects of NaOH Concentration on Zeolite Synthesis from Fly Ash with a Hydrothermal Treatment Method, 24(24), 183–191.

[18] Murat, M., Amokrane, A., Bastide, J. P., & Montanaro, L. (1992). Synthesis of zeolites from thermally activated kaolinite. Some observations on nucleation and growth. Clay Minerals, 27, 119–130.

[19] Alkan, M., Hopa, C., Yilmaz, Z., & Guler, H. (2005). The effect of alkali concentration and solid / liquid ratio on the hydrothermal synthesis of zeolite NaA from natural kaolinite. Microporous and Mesoporous Materials, 86, 176–184.

[20] Masters, A. F., & Maschmeyer, T. (2011). Zeolites - From curiosity to cornerstone. Microporous and Mesoporous Materials, 142(2–3), 423–438.

[21] Novembre, D., Sabatino, B. Di., Gimeno, D., Garcia-Vallès, M., Martínez, S. (2004). Synthesis of Na–X zeolites from tripolaceous deposits (Crotone, Italy) and volcanic zeolitised rocks (Vico volcano, Italy). Microporous and Mesoporous Materials 75(1-2):1-11.

[22] Akolekar, D., Chaffee, A., Howe, R. F., (1997). The transformation of kaolin to low silica X zeolite. Zeolites, 19(5), 359–365.

[23] Chandrasekhar, S. (1996). Influence of Metakaolinization Temperature on the formation of zeolite 4A from kaolin. Clay Minerals, 31, 253–261.